

Electronic Supplementary Information

**Inducible epitope imprinting : ‘Generating’ the required binding site
in membrane receptor for targeted drug delivery**

Sha Liu,^a Qiuyan Bi,^a Yingying Long,^a Zhuoxuan Li,^a Sanjib Bhattacharyya,^b

Chong Li^{*a}

^a College of Pharmaceutical Sciences, Key Laboratory of Luminescence and Real-time Analytical Chemistry (Ministry of Education), Southwest University, Chongqing, 400716, China

^b WPI-AIMR, Tohoku University, Sendai, Japan

* To whom correspondence should be addressed.

E-mail: chongli@swu.edu.cn

Electronic Supplementary Information

Abbreviations	2
Materials	3
Experimental details	4
Peptide synthesis and characterization	4
Preparation of nanoparticles	4
Characterization of MIPNP-F	5
Circular dichroism (CD) spectroscopy	5
Interaction between MIPNP and target protein	6
MIPNP and target cell binding assay	6
Uptake of MIPNP by target cells (in vitro targeting capability)	7
Uptake-mechanism study	7
Cytotoxicity study of NPs	7
Establishment of tumor-bearing animal models	8
In vivo imaging assay	8
In vivo tissue distribution assay	8
In vivo antitumor study performed using PDT	9
Primary test of potential toxicity	9
References	9
Supporting table and figures	10

Abbreviations

MIP: Molecularly imprinted polymer

NP: Nanoparticle

FA: Folic acid

FR α : Folate receptor- α

FN peptide: FR α N-terminal peptide

FA-NP: Folate polyacrylamide NP

MIPNP: Molecularly imprinted polymeric NP

NIPNP: Non-imprinted NP

MIPNP-A: Synthetic polymeric NP prepared using apamin peptide as the imprinting template

MIPNP-L: Synthetic polymeric NP prepared using linear apamin as the imprinting template

MIPNP-F: Synthetic polymeric NP prepared using FN peptide as the imprinting template

MIPNP-S: Synthetic polymeric NP prepared using scrambled FN peptide as the imprinting template

FOA: Fluorescein o-acrylate

NIL: Nile red, 9-(diethylamino)benzo[a]phenoxazin-5(5H)-one

FITC: Fluorescein isothiocyanate

MB: Methylene blue

DOX: Doxorubicin

IR-783: 2-[2-[2-Chloro-3-[2-[1,3-dihydro-3,3-dimethyl-1-(4-sulfobutyl)-2H-indol-2-ylidene]-ethylidene]-1-cyclohexen-1-yl]-ethenyl]-3

DAPI: 4',6'-Diamidino-2-phenylindole

C6: Coumarin 6

MTT: 3-(4,5-Dimethylthiazol-2-yl)-2,5-diphenyltetrazolium bromide

PDT: Photodynamic therapy

IC: Ion chromatography

CD: Circular dichroism

TEM: Transmission electron microscopy

FP: Fluorescence polarization

OD: Optical density

H&E: Hematoxylin and eosin

AAm: Acrylamide

BIS: N,N'-methylenebisacrylamide

TFMA: 2-(Trifluoromethyl)acrylic acid

TFEA: 2,2,2-Trifluoroethyl acrylate

APMA: N-(3-aminopropyl) methacrylamide hydrochloride

APS: Ammonium persulfate

TEMED: N,N,N,N-tetramethylethylenediamine

TFE: 2,2,2-Trifluoroethanol

EtOH: Ethyl alcohol

Materials

The following materials were obtained from commercial sources: acrylamide (AAm), N,N'-methylenebisacrylamide (BIS), ammonium persulfate (APS), 2-(trifluoromethyl) acrylic acid (TFMA), 4',6'-diamidino-2-phenylindole dihydrochloride (DAPI), monensin, and fluorescein isothiocyanate (FITC), from Aladdin (Shanghai, China); N-(3-aminopropyl) methacrylamide hydrochloride (APMA), from Accela ChemBio Co. Ltd. (Shanghai, China); N,N,N,N-tetramethylethylenediamine (TEMED), from ACROS (Beijing, China); Nile red (NIL) and folic acid (FA), from Macklin (Shanghai, China); fluorescein o-acrylate (FOA), filipin, and chlorpromazine, from Sigma (St. Louis, MO, USA); recombinant folate receptor- α (FR α) protein, recombinant protein P32 and Fn14, from Sino Biological Inc. (Beijing, China); brefeldin A (BFA), from Selleckchem (Huston, TX, USA); 3-(4,5-Dimethylthiazol-2-yl)-2,5-diphenyltetrazolium bromide (MTT), from Notlas Biology Technical Co. Ltd. (Beijing, China); methylene blue (MB), from Kelong Chemical Co. Ltd. (Beijing, China); methyl- β -cyclodextrin and colchicine, from Dingguo Changsheng Biotechnology Co. Ltd. (Beijing, China); and 2,2,2-trifluoroethyl acrylate (TFEA) from Tokyo Chemical Industry Development Co. Ltd. (Tokyo, Japan). All other chemicals were of analytical grade.

We purchased HeLa human cervical-cancer cells, A549 human lung adenocarcinoma epithelial cells, PANC-1 human pancreatic-cancer cells, and MCF7 human breast-cancer cells from KeyGEN Biology Co. (Nanjing, China). A human nasopharyngeal carcinoma cell line, KB, was a gift from the School of Pharmacy, Fudan University. All cells were grown in Dulbecco's modified Eagle's medium (DMEM) containing 10% (v/v) heat-inactivated fetal bovine serum (FBS), 100 U·mL⁻¹ penicillin, and 100 μ g·mL⁻¹ streptomycin. Cultures were maintained under a humidified atmosphere of 5% CO₂ at 37°C.

BALB/c nude mice (4–6 weeks old) were obtained from Shanghai SLAC Laboratory Animal Co. Ltd. (Shanghai, China), and maintained under specific pathogen-free (SPF) conditions. All animal experiments were performed in accordance with guidelines approved by the ethics committee of the College of Pharmaceutical Sciences, Southwest University, Chongqing, P.R. China.

Experimental Section

Peptide synthesis and characterization

Peptides were synthesized by means of solid-phase peptide synthesis performed using Fmoc-protected amino acids, following which reversed-phase HPLC was used to purify the peptides to homogeneity. Peptide purity and molecular weight were ascertained by performing analytical HPLC and ESI mass spectrometry. The peptide sequences were as follows:

Apamin peptide: CNCKAPETALCARRCQQH-NH₂

Linear apamin peptide: ANAKAPETALAARRAQQH-NH₂

FN peptide: Ac-QTRIAWARTELLNVAMNAKH

Scrambled FN peptide: Ac-RIWKQTELWNATLNHRAAVA

Preparation of nanoparticles (NPs)

The NPs molecularly imprinted with FN peptide (MIPNP-F) were prepared using the precipitation polymerization reaction.¹ Briefly, AAm (27 mg), TFMA (18 mg), and BIS (6 mg) were dissolved by sonicating in 2.5 mL of ultrapure water, and then TFEA (6 mg) and FN peptide were dissolved in 2.5 mL of TFE/EtOH and maintained for a few minutes before addition to the monomer solution. The mixture was degassed in a sonication bath under vacuum for 10 min and agitated for 30 min under nitrogen atmosphere at room temperature. Polymerization was initiated by adding APS (60 mg·mL⁻¹, 150 μ L) and TEMED (10 μ L) under vacuum protection and the mixtures were stirred for 20 h. Lastly, ethanol was added to the polymerized solutions to precipitate the NPs, which were then centrifuged at 8000 rpm for 15 min. This process was repeated thrice to remove the template, surfactants, and unreacted monomers. The collected sediment was redissolved in ultrapure water, and then purified using a Sephadex G-50 column and lyophilized for further use. The NPs molecularly imprinted with scrambled FN peptide (MIPNP-S) were prepared by the same method, except that FN peptide was replaced with the scrambled FN peptide. Non-imprinted NPs (NIPNPs) were synthesized in an identical manner, except that no peptide was added.

The NPs imprinted using apamin (MIPNP-A) and linear apamin (MIPNP-L) as templates were synthesized by following the same steps as those used for MIPNP-F, except that the monomers used were AAm (35.5 mg) and BIS (11.5 mg) and the peptides were replaced with apamin or linear apamin.

The folated polyacrylamide NP (FA-NP) was prepared as follows: First, amino NP was synthesized using the aforementioned methods, except that APMA (1 mg) was added as part of the monomers.² Next, FA was conjugated on the amino NP through EDC chemistry: FA and EDC-NHS were dissolved in DMSO and magnetically stirred for 2 h at room temperature in the dark, following which amino NP dissolved in ultrapure water was added into this reaction mixture and magnetically stirred for 24 h under the same conditions. Subsequently, the as-prepared FA-NP solution was

dialyzed against ultrapure water for 48 h and centrifuged at 10000 rpm for 10 min to remove free FA. Lastly, the products were lyophilized for further use.³

NIL-loaded, C6-loaded, FOA-loaded, IR-783-loaded, and MB-loaded NPs were synthesized by adding NIL, C6, FOA, IR-783, and MB, respectively.

Characterization of MIPNP-F

The morphology of NIPNP and MIPNP-F was observed using a thermal field emission scanning electron microscope (TF-SEM; JSM-6700F, JEOL, Japan) with an accelerated voltage of 10.0 kV. (Figure S2) Transmission electron microscopy (TEM; JEM-100CX, JEOL, Japan) was also used for morphological examination of MIPNP-F after negative-staining with sodium phosphotungstate solution. Briefly, NPs were dissolved in ultrapure water and pipetted onto a carbon-coated copper grid. After air-drying, the samples were examined in the bright-field mode, at an operating voltage of 200 kV. The hydrodynamic diameter of MIPNP-F was determined in aqueous solution ($1 \text{ mg} \cdot \text{mL}^{-1}$) using a Zetasizer Nano ZS (Malvern, Worcestershire, UK). The temperature was controlled at $25^\circ\text{C} \pm 0.1^\circ\text{C}$. Each sample was measured at least 3 times (Figure S3).

To determine the fluorine percentage in MIPNP-F, we used oxygen combustion in closed systems combined with ion chromatography (IC) methods.^{4,5} Briefly, NPs were weighed precisely and wrapped in filter paper. Ultrapure water was used as the absorbent in the flask. The filter paper was set in the combustion flask and impregnated with 1–2 drops of acetone, following which combustion was performed. After combustion, the absorbent was transferred into a test tube and the inside of the flask was washed out with ultrapure water and divided into 3 parts. The IC experiments were performed on an IC system (ICS-1100, Dionex, USA) operating in a double-column mode with conductometric detection in the isothermal regime. The samples were eluted with a mixture of 2 mM Na_2CO_3 and 3 mM NaHCO_3 solutions at an elution rate of $3 \text{ mL} \cdot \text{min}^{-1}$; the sample volume was 0.1 mL. The analytical column AS23 (Dionex, USA) was used in this assay (Figure S3).

The concentration of MIPNP-F was measured using a qNano instrument (Izon Science Ltd., Burnside, New Zealand) at 25°C .⁶ In this system, tunable nanopores and propriety data-capturing software (Izon Control Suite v3.1.2.5) are used. Briefly, NP400 nanopore was selected to measure NP concentrations in serial-dilution samples and obtain more reliable data membranes. We counted at least 500 events per sample. Calibration was performed using calibration beads of a defined concentration (provided by Izon) (Figure S3).

Circular dichroism (CD) spectroscopy

Room-temperature CD spectra of peptides were measured from 190 to 250 nm on a Bio-Logic (MOS 500) spectropolarimeter using a quartz cuvette (path length: 1 mm). CD spectra of FN peptides ($0.2 \text{ mg} \cdot \text{mL}^{-1}$) were measured in water, TFE (50%, v/v),

EtOH (50%, v/v) (Figures S1, S22A). To study the inducement effect of MIPNPs on the secondary structure of the peptide, MIPNPs of different concentrations were pre-examined using the CD spectrometer (Figures S4), and then, MIPNPs (2 mg·mL⁻¹) were added to the peptide (0.2 mg·mL⁻¹) and co-incubated for 2 h at room temperature before CD spectra of peptides were measured (Figures 1A, 2A, S22B).

Interaction between MIPNP and target protein

We used the fluorescence-polarization (FP) technique to study the direct interactions between MIPNP-F and recombinant FR α protein. FITC-conjugated FR α (FITC-FR α) was synthesized and purified using the NHS-Fluorescein antibody-labeling kit from Pierce (Appleton, USA). In the FP experiments, the fluorophore was examined using a microplate reader (Infinite 200 Pro, Tecan, Switzerland) equipped with 485-nm excitation and 535-nm emission filters. The FP value (P) was defined as a function of the observed parallel intensity (I_{\parallel}) and perpendicular intensity (I_{\perp}): $P = (I_{\parallel} - I_{\perp}) / (I_{\parallel} + I_{\perp})$.

FP dose-response analysis of the interaction of FITC-FR α with NPs was performed at 37°C in the dark. Briefly, MIPNP-F, MIPNP-S, and NIPNP dissolved in PBS (0.01 M, pH 7.4) at various concentrations were separately incubated with FITC-FR α (0.1 μ g·mL⁻¹) for 2 h. A curve was generated from the measured FP values and the interaction KD was calculated by using GraphPad Prism 5 software with the non-linear regression option “Binding saturation: total and nonspecific binding”. Recombinant protein P32 and Fn14 were used as control in this assay (Figures 1B, 2B, S6, S22C).⁷

The emission wavelength (λ_{em}) of tryptophan residue of FN peptide was measured on the spectrofluorometer (F-7000, Hitachi, Japan) using a 0.3 cm path length cuvette. MIPNPs (2 mg·mL⁻¹) were added to the FN-peptide (0.2 mg·mL⁻¹) and co-incubated for 2 h at room temperature. Excitation of 280 nm was used and emission scans ranged from 410 nm to 300 nm. Excitation and emission slit widths were of 2.5 nm and 5.0 nm, respectively. An average time of 1.0 second was used (Figure S5).

MIPNP and target cell binding assay

The real-time NP-cell interaction was monitored at 37°C by using Ligand Tracer Green (Ridgeview Instruments AB, Uppsala, Sweden).⁸ HeLa or A549 cells were seeded on a local part of a cell dish and cultivated until the cell number was approximately 10⁶. All measurements were conducted in 3 mL of cell-culture medium and started with a short baseline, and this was followed by a 5-step uptake study performed using increasing concentrations of FOA-loaded NPs. Next, a retention measurement was performed in fresh cell-culture medium (Figures 3A, S7). Data were evaluated and the equilibrium KD was estimated using TraceDrawer 1.3 software (Ridgeview Instruments AB) and a one-to-one binding model (Table S1).

Uptake of MIPNP by target cells (in vitro targeting capability)

HeLa, KB, and PANC-1 cells, which are known to vastly overexpress FR α , were used to study the targeting ability of MIPNP-F. Briefly, HeLa, KB, and PANC-1 cells were separately plated in 24-well plates in DMEM containing 10% FBS at a density of 5×10^4 cells per well and cultured for 24 h. NIL-loaded NPs (MIPNP-F, MIPNP-S, NIPNP; $4 \text{ mg} \cdot \text{mL}^{-1}$) were added into the plates and incubated for 2 h, following which the cells were washed with PBS (0.1 M, pH 7.4), fixed with paraformaldehyde, and stained with DAPI. Fluorescence images of the cells were obtained using a fluorescence microscope (IX73, Olympus, Japan) (Figures 3B, S8). The fluorescence intensity of cells treated with various NP samples was also measured using flow cytometry (ACEA Novo Cyte, 2060R); the flow velocity was $14 \text{ } \mu\text{L} \cdot \text{min}^{-1}$, and the diameter of the sample flow was $7.7 \text{ } \mu\text{m}$. Cell-associated NIL was excited with an argon laser (488 nm), and fluorescence was detected at 580 nm (Figures S9-S10). To further investigate the specific targeting ability of MIPNP-F, we also tested two cell lines with low FR expression: A549 and MCF7.

To examine the potential influence of serum FA on the targeting ability of MIPNP-F, we conducted a preliminary analysis on HeLa cells as follows: HeLa cells were seeded in 24-well plates and cultured at 37°C with 5% CO_2 , and after 24-h cultivation, the cells were preincubated with medium containing FA (0, 1, 10, $100 \text{ } \mu\text{g} \cdot \text{mL}^{-1}$) for 30 min. Next, MIPNP-F ($4 \text{ mg} \cdot \text{mL}^{-1}$) was added to cells, and after culturing for 2 h at 37°C , the cells were stained with DAPI and examined using both fluorescence microscopy (Figure S12) and flow cytometry (Figure 3C). The experiment was also conducted using the same methods and FA-NP as a control (Figures S11, S12).

Uptake-mechanism study

To investigate the mechanism of MIPNP-F uptake, HeLa cells were preincubated for 30 min (in 24-well plates) with various endocytosis inhibitors: chlorpromazine ($20 \text{ } \mu\text{g} \cdot \text{mL}^{-1}$), filipin ($5 \text{ } \mu\text{g} \cdot \text{mL}^{-1}$), colchicine ($400 \text{ } \mu\text{g} \cdot \text{mL}^{-1}$), BFA ($7.5 \text{ } \mu\text{g} \cdot \text{mL}^{-1}$), and monensin ($1.25 \text{ } \mu\text{g} \cdot \text{mL}^{-1}$). Next, NIL-loaded NPs (MIPNP-F, FA-NP, NIPNP; $4 \text{ mg} \cdot \text{mL}^{-1}$) were added and incubated for 1 h. Energy-dependence experiments were performed by incubating NPs with the cells at 4°C for 1 h.⁹ Lastly, cells were washed thrice with PBS (0.1 M, pH 7.4), and then quantitative data were obtained using flow cytometry (Figures 3D, S13).

Cytotoxicity study of NPs

The cytotoxicity of NPs loaded with the photosensitizer methylene blue (MB) was examined using photodynamic treatment (PDT) and measured by the MTT assay. HeLa cells were seeded in 96-well plates at a density of 5×10^3 cells per well and cultured for 24 h. MB-loaded NPs (MIPNP-F, MIPNP-S, NIPNP) were diluted to predetermined concentrations with PBS and added into each well, and after incubation for 2 h at 37°C , the medium was refreshed. Next, PDT was performed using 650-nm laser light, at a power density of $50 \text{ mW} \cdot \text{cm}^{-2}$ for 12 min, and 30 min later, $20 \text{ } \mu\text{L}$ of MTT ($5 \text{ mg} \cdot \text{mL}^{-1}$ in PBS) was added into each well and incubated for 4 h at 37°C .

Lastly, the medium was replaced with 150 μL of DMSO, the optical density (OD) at 490 nm was measured using a microplate reader (Bio-Rad, USA), and cell viability was calculated. The dark (no PDT) toxicity of MB-loaded NPs was analyzed using the same method (Figure S18).

Establishment of tumor-bearing animal models

All animal experiments were performed in accordance with guidelines approved by the ethics committee of the College of Pharmaceutical Sciences, Southwest University. The subcutaneous tumor models were established through subcutaneous injection of HeLa cells (5×10^6) or A549 cells (8×10^6) into the right flanks of BALB/c nude mice. The mice were then reared under standard conditions, and tumor volumes were calculated using this formula: tumor volume = $[\text{length} \times (\text{width})^2]/2$; the length and the width of each tumor were measured using Vernier calipers. The mice were used in experiments after the tumors had grown to a size of 50–120 mm^3 .

In vivo imaging assay

The nude mice bearing the HeLa-cell tumors were randomly divided into 3 groups and treated with IR783-loaded NPs: MIPNP-F, MIPNP-S, or NIPNP; the treatment was performed by intravenously administering 100 μL of the NPs ($10 \text{ mg} \cdot \text{kg}^{-1}$). All mice were examined using an in vivo imaging system (FX-Pro, Carestream, USA) at predetermined time points (2, 4, 8, 12, and 24 h). Lastly, the mice were sacrificed through intracardiac perfusion with PBS, and the tumors, hearts, livers, spleens, lungs, and kidneys were collected and imaged using the in vivo imaging system (Figures 4A, 4B). The A549 tumor-bearing nude mice were also studied using this assay (Figures S14, S15).

To study the potential influence of free FA on the in vivo tumor targeting ability of NPs, free FA ($1 \mu\text{g} \cdot \text{mL}^{-1}$, 50 μL) was pre-injected near the tumor of mice models and 0.5 h later, IR783-loaded MIPNP-F or FA-NP ($10 \text{ mg} \cdot \text{kg}^{-1}$) was administered via tail vein. Whole body in-vivo images were taken at predetermined time points. Besides, mouse organs, including tumor, liver, spleen, kidneys, heart, and lung, were harvested and imaged using the in vivo imaging system at 2, 4, 8, 12, 24 h, respectively (Figure S16).

In vivo tissue distribution experiment

The HeLa tumor bearing nude mice were randomly divided into three groups (6 mice per group), and treated with C6-loaded nanoparticles (MIPNP-F, MIPNP-S, NIPNP) via tail vein, respectively. At 24 h post-injection, mice were sacrificed, and tumors were collected. The tumors were weighed and homogenized in saline and the C6 fluorescein was extracted by ethyl acetate, then quantified by Microplate Reader (Infinite 200 Pro, Tecan, Switzerland) (Figure 4C).

To quantitatively determined the influence of free FA on the in vivo tumor targeting ability of NPs, the HeLa-tumor-bearing nude mice were divided into four groups (6 mice per group), free FA ($1 \mu\text{g} \cdot \text{mL}^{-1}$, 50 μL) was pre-injected near the tumor of mice

models and 0.5 h later, C6-loaded nanoparticles (MIPNP-F, MIPNP-S, NIPNP) were administered via tail vein. In each group, mice were sacrificed at 2, 4, 8, 12, 24 h post injection, and tumors and tissues were collected. The collected samples were homogenized in saline, extracted by ethyl acetate, and quantified by Microplate System (Infinite 200 Pro, Tecan, Switzerland) (Figure S17).

In vivo antitumor study performed using PDT

We randomly divided 18 nude mice bearing subcutaneous HeLa-cell tumors into 3 groups (6 mice per group), and treated the mice with MB-loaded MIPNP-F (50 mg·mL⁻¹, 100 μL), MB-loaded NIPNP (50 mg·mL⁻¹, 100 μL), or PBS (0.1 M, pH 7.4). All samples were intravenously injected through the tail vein on Day 0 and Day 5, and then at 12 and 24 h post-injection each time, the tumor sites were treated with 650-nm laser light at a power density of 800 mW·cm⁻² for 10 min. The longest and the shortest diameters of the tumors were measured, recorded, and analyzed at predetermined time points (Figure S19).

Primary test of potential toxicity

To evaluate the in vitro cytotoxicity of MIPNP-F, cell viability was measured by the MTT assay. HeLa cells were seeded in 96-well plates at a density of 5×10^3 cells per well, and after 24 h, MIPNP-F at various concentrations (1, 5, 10, 15, 20 mg·mL⁻¹) was added into the wells and incubated at 37°C. After incubation for 48 h, 20 μL of MTT (5 mg·mL⁻¹ in PBS) was added into each well and incubated for 4 h at 37°C, following which the culture medium was removed, 150 μL of DMSO was added and mixed for 15 min in the dark at room temperature, and the OD₄₉₀ was measured using a microplate reader (Bio-Rad). Cell viability was calculated as the percentage of the OD of treated cells relative to that of control cells (Figure S20).

To measure in vivo toxicity, MIPNP-F (50 mg·mL⁻¹, 100 μL) was intravenously injected into mice on Days 0 and 5. The control-group mice were injected (in parallel) with an equal volume of PBS (0.1 M, pH 7.4). At 10 days post-injection, the mice were sacrificed, and sections of heart, liver, spleen, lung, and kidney tissues were stained with hematoxylin and eosin (H&E) and examined using an optical microscope (Figure S21).

References

1. Y. Hoshino, T. Kodama, Y. Okahata, K. J. Shea, *J. Am. Chem. Soc.* 2008, **130**, 15242-15243.
2. M. Qin, H. J. Hah, G. Kim, G. Nie, Y. E. Lee, R. Kopelman, *Photochem. Photobiol. Sci.* 2011, **10**, 832-841.
3. W. Wang, C. Y. Tong, B. Liu, X. Y. Liu, T. Liu, *J. Control. Release* **2015**, **22**, 3311-3317.
4. T. Myahara, F. Ogai, H. Kitamura, K. Narita, Y. Takino, T. Toyooka, *Anal. Sci.* 1998, **14**, 1145-1147.
5. E. F. Safonova, V. F. Selemenev, T. A. Brezhneva, A. I. Slivkin, *Pharm. Chem. J.* 1999, **33**, 622-623.
6. F. Varenne, A. Makky, M. Gaucher-Delmas, F. Violleau, C. Vauthier, *Pharm. Res.* 2016, **33**, 1220-1234.
7. J. Jiang, Y. Zhang, A. R. Krainer, R. Xu, *Proc. Natl. Acad. Sci. U. S. A.* **1996**, **96**, 3572-3577.
8. L. Ekerljung, H. Wällberg, A. Sohrabian, K. Andersson, M. Friedman, F. Frejd, S. Ståhl, L. Gedda, *Bioconjugate Chem.* 2012, **23**, 1802-1811.
9. S. Bhattacharyya, R. D. Singh, R. Pagano, J. D. Robertson, R. Bhattacharya, P. Mukherjee, *Angew. Chem. Int. Ed.* 2012, **51**, 1563-1567.

Supporting table and figures

Table S1. Kinetic data from the binding assay performed using live cells.

		MIPNP-F	MIPNP-S	NIPNP
HeLa	K _{on} (M)	2.59E4 (±1.17E2)	1.94E2 (±9.14E-1)	2.74E2 (±1.33E-1)
	K _{off} (M)	7.28E-4 (±1.46E-6)	6.13E-3 (±8.81E-5)	5.81E-3 (±1.02E-5)
	KD (M)	2.81E-8 (±5.81E-10)	3.14E-5 (±1.74E-7)	2.15E-5 (±3.05E-7)
A549	K _{on} (M)	7.65E1 (±3.55E-1)	6.64E1 (±5.48E-1)	5.36E1 (±5.85E-1)
	K _{off} (M)	2.85E-3 (±3.48E-5)	3.69E-3 (±5.58E-5)	1.57E-3 (±4.9E-5)
	KD (M)	3.73E-5 (±2.27E-7)	5.71E-5 (±1.75E-7)	2.92E-5 (±6.58E-7)

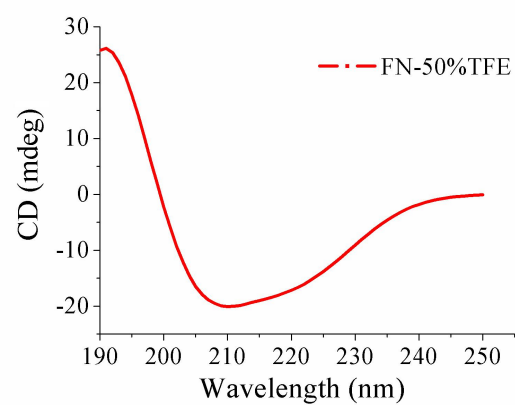


Figure S1. CD spectrum of FN peptide in 50% TFE/water at 25°C.

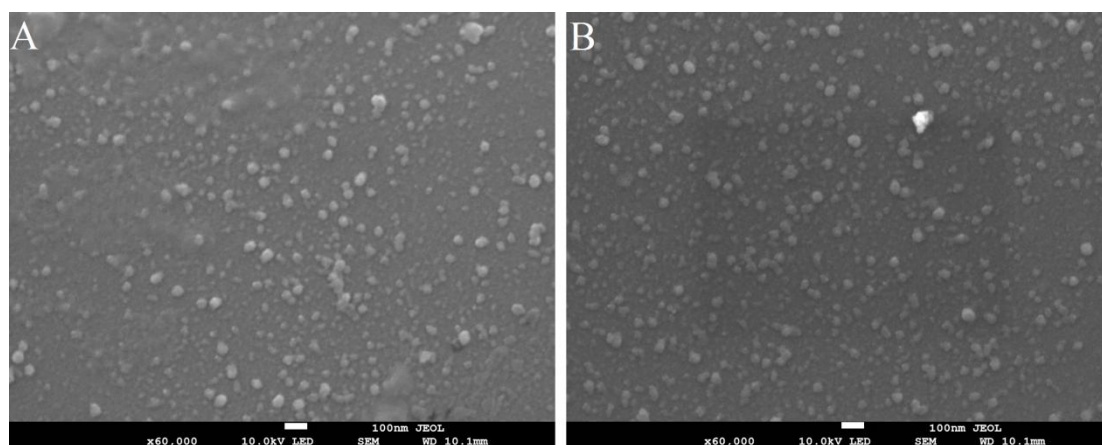


Figure S2. The morphology of nanoparticles observed by SEM. A:MIPNP-F; B: NIPNP.

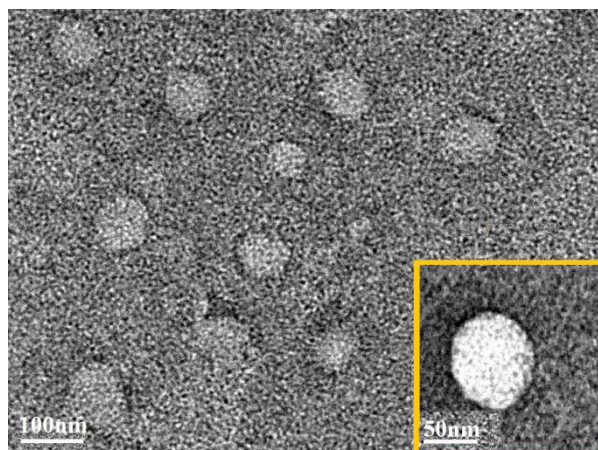


Figure S3. Transmission electron microscopy image of MIPNP-F. The particle size of MIPNP-F measured using dynamic light scattering was 78 nm. The atomic percentage of the element F in MIPNP-F was 7.28%, which was measured using oxygen combustion in closed systems combined with ion-chromatography methods. The concentration of MIPNP-F was $2 \times 10^{-13} \text{ mol} \cdot \text{mL}^{-1}$ (measured using qNano).

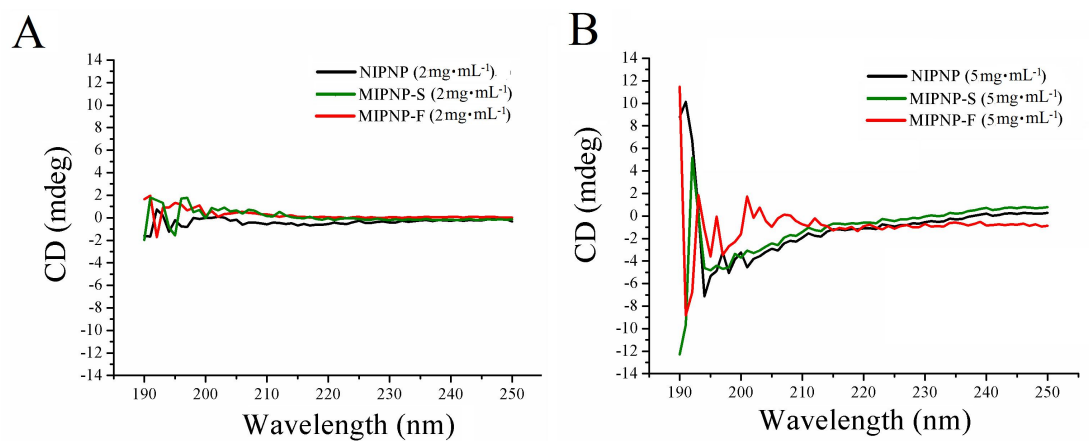


Figure S4. CD spectra of blank nanoparticles (MIPNP-F, MIPNP-S, NIPNP) in PBS at 25°C.

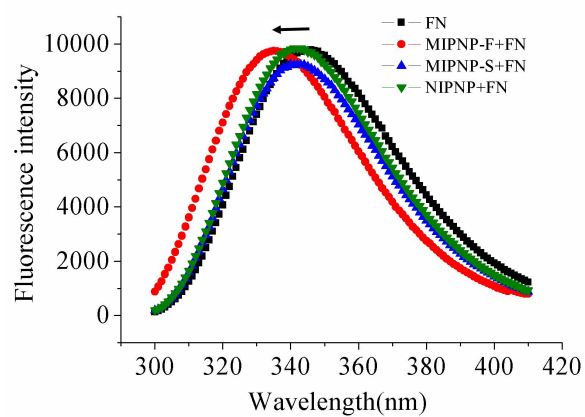


Figure S5. The tryptophan fluorescence wavelength of FN peptide measured in the absence or presence of NPs.

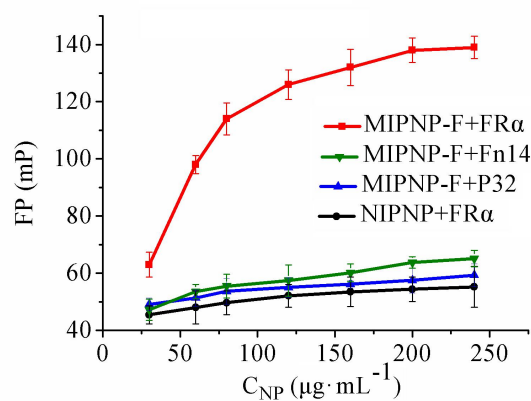


Figure S6. Fluorescence-polarization analysis of direct binding between NPs and FITC-labeled recombinant protein. The N-terminal of P32 is α -helix, and that of Fn14 is flexible in conformation. The molecular weight of both Fn14 (Mw=34 kDa) and P32 (Mw= 19 kDa) are roughly equal to that of FR α (Mw=26 kDa). The KD of MIPNP-F binding with FR α was calculated to be 5.72 nM.

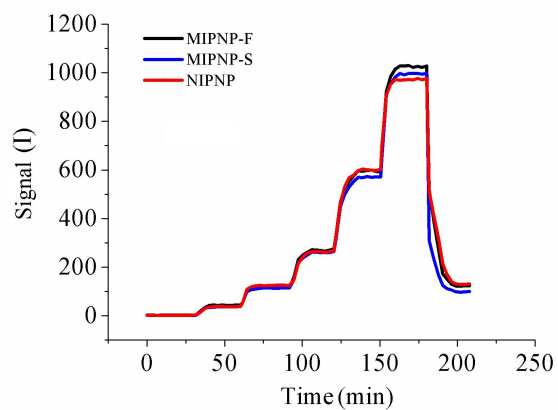


Figure S7. Binding curves showing the real-time interaction of FOA-loaded NPs at various concentrations with A549 cells (low expression of FR), measured using Ligand Tracer.

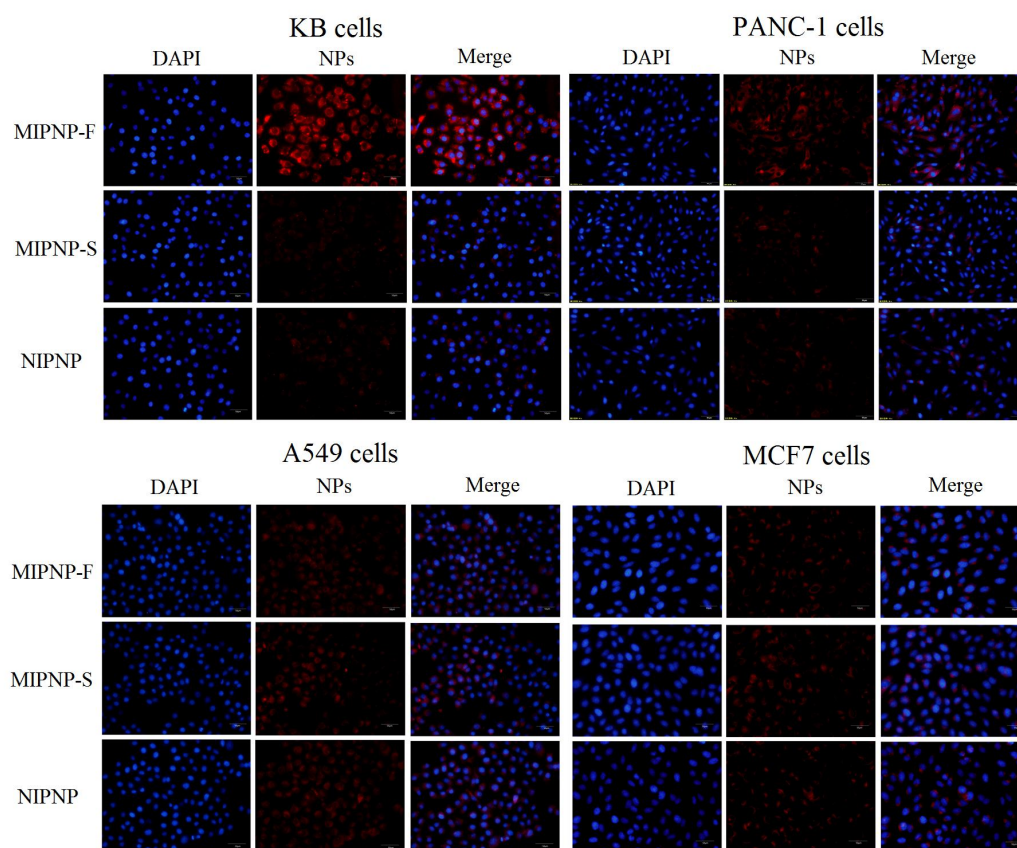


Figure S8. In vitro cellular uptake study. Fluorescence images showing uptake of NIL-loaded NPs by KB and PANC-1 cells (high expression of FR) and A549 and MCF7 cells (FR low expression of FR). Red fluorescence indicates NIL uptake.

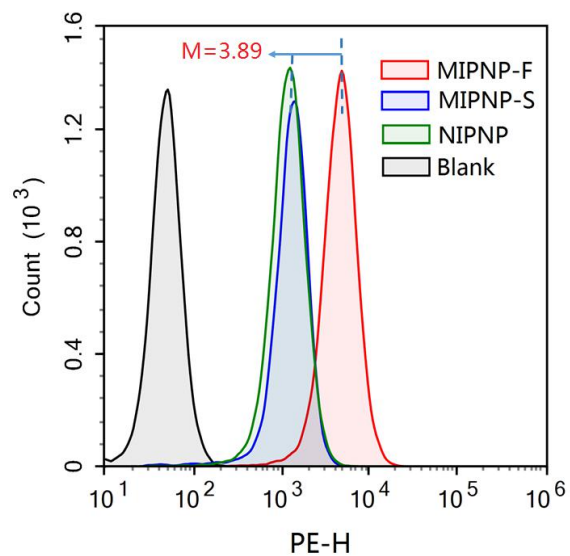


Figure S9. Flow cytometric measurement of the uptake of NIL-loaded NPs by HeLa cells. Blank (black curves): the cells alone; M: fluorescence intensity ratio, MIPNP-F-treatment group to NIPNP-treatment group.

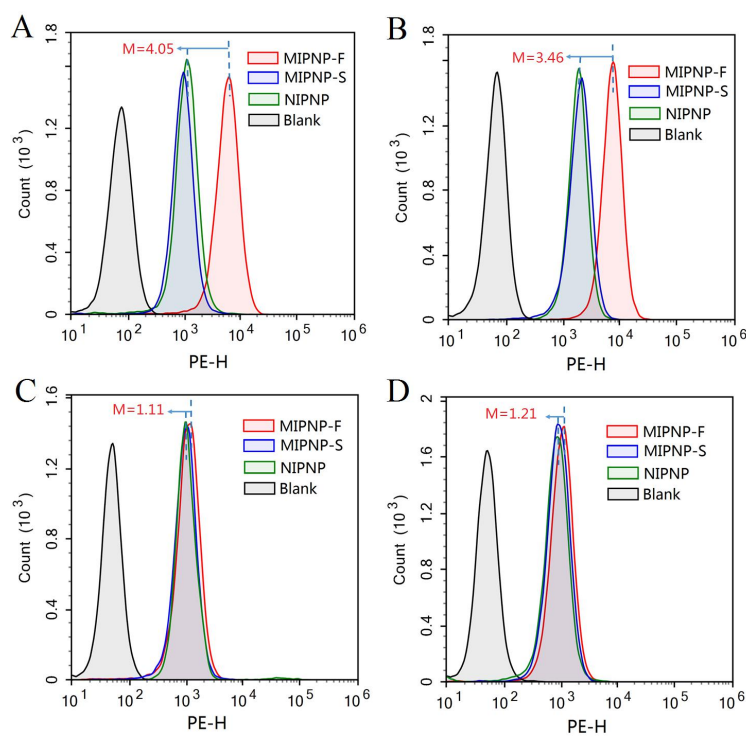


Figure S10. Flow cytometric measurement of the uptake of NIL-loaded NPs by different cell types. A: KB cells (high expression of FR); B: PANC-1 cells (high expression of FR); C: A549 cells (low expression of FR); and D: MCF7 cells (low expression of FR). Blank (black curves): the cells alone; M: fluorescence intensity ratio, MIPNP-F-treatment group to NIPNP-treatment group.

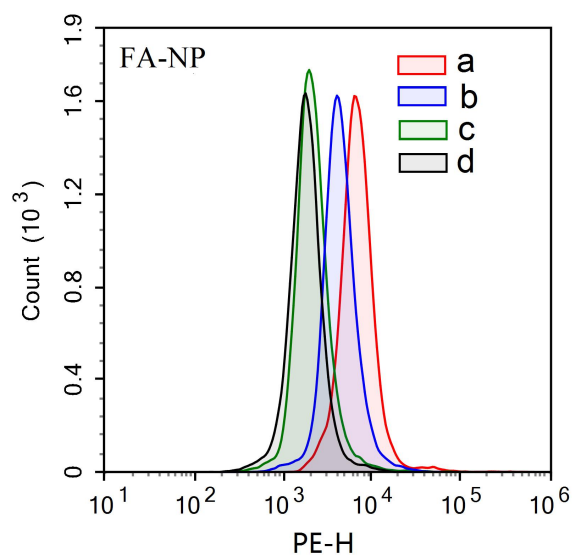


Figure S11. Potential influence of serum FA on the targeting ability of FA-NP, studied using flow cytometry. FA at different concentrations was incubated with HeLa cells for 30 min at 37°C and then FA-NP was added to the cells, which were subsequently examined by flow cytometry. a: 0 $\mu\text{g}\cdot\text{mL}^{-1}$ FA; b: 1 $\mu\text{g}\cdot\text{mL}^{-1}$ FA; c: 10 $\mu\text{g}\cdot\text{mL}^{-1}$ FA; and d: 100 $\mu\text{g}\cdot\text{mL}^{-1}$ FA.

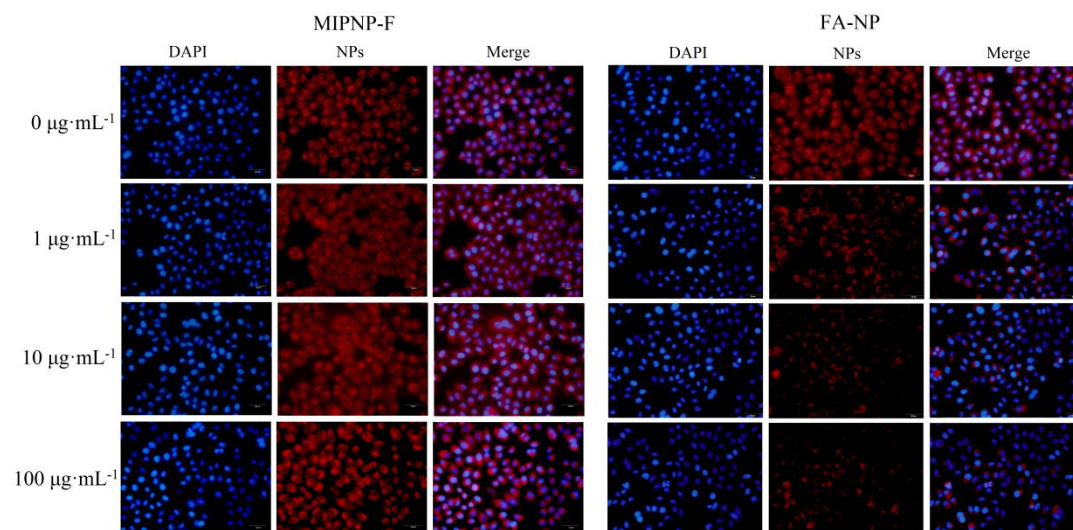


Figure S12. Potential influence of serum FA on the targeting ability of MIPNP-F, examined using fluorescence microscopy. FA at indicated concentrations was incubated with HeLa cells for 30 min at 37°C, and then MIPNP-F or FA-NP was added to the cells, which were subsequently examined using fluorescence microscopy.

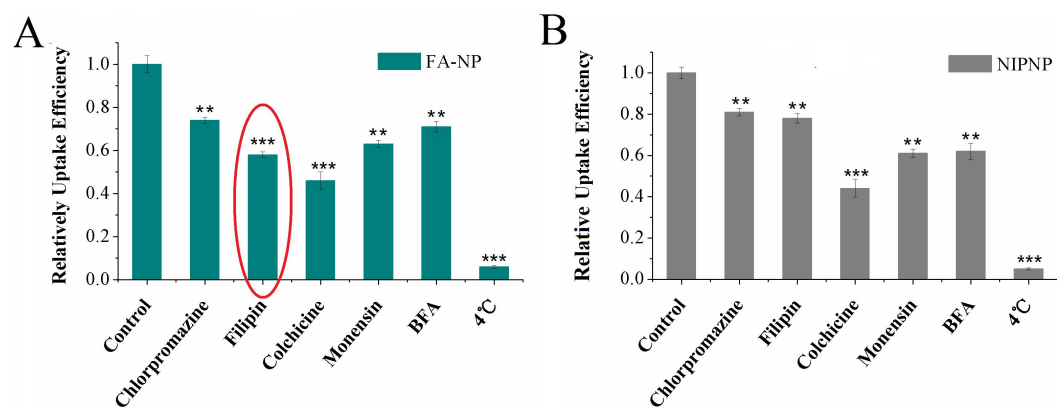


Figure S13. Analysis of the mechanism of uptake of NIL-loaded FA-NP and NIPNP by HeLa cells. ** $p < 0.01$ and *** $p < 0.005$ versus control group.

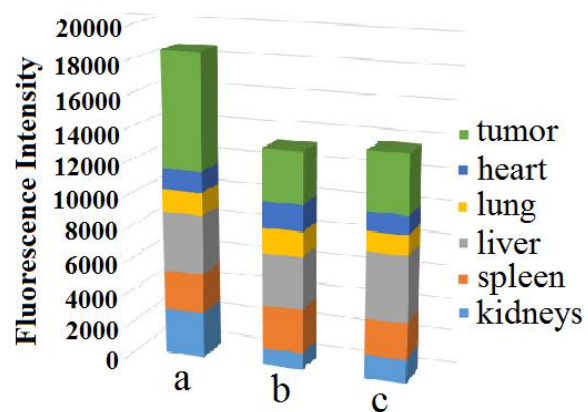


Figure S14. Semiquantitative results obtained using ex vivo fluorescence images by in vivo NP distribution assay in HeLa-tumor-bearing nude mice. a: MIPNP-F; b: MIPNP-S; c: NIPNP.

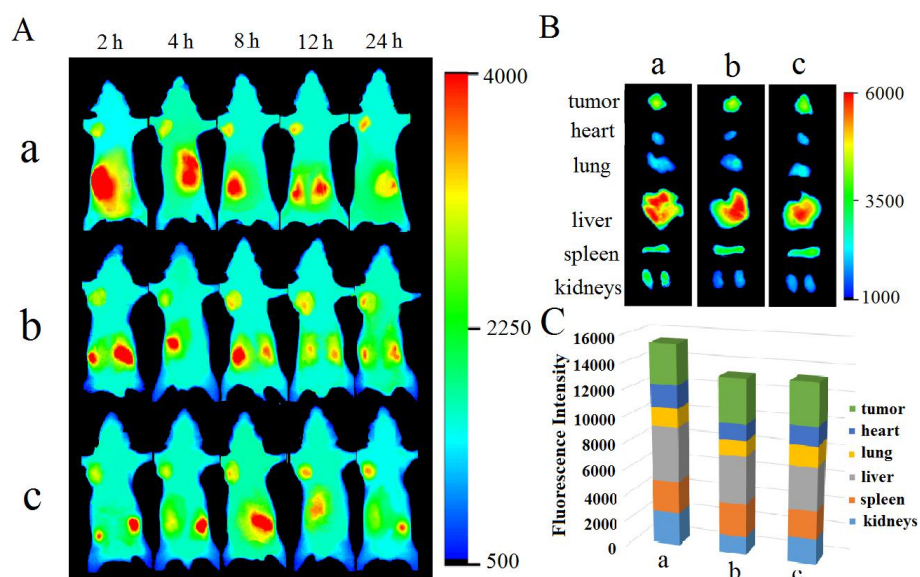


Figure S15. In vivo NP distribution in A549-tumor-bearing nude mice. (A) The model mice were intravenously injected with NPs (100 μ L, 10 mg \cdot kg $^{-1}$) and examined using an in vivo imaging system at indicated time points. (B) Fluorescence images of major organs and tumors ex vivo at 24 h post-injection. (C) Semiquantitative results obtained using ex vivo fluorescence images. a: MIPNP-F; b: MIPNP-S; c: NIPNP.

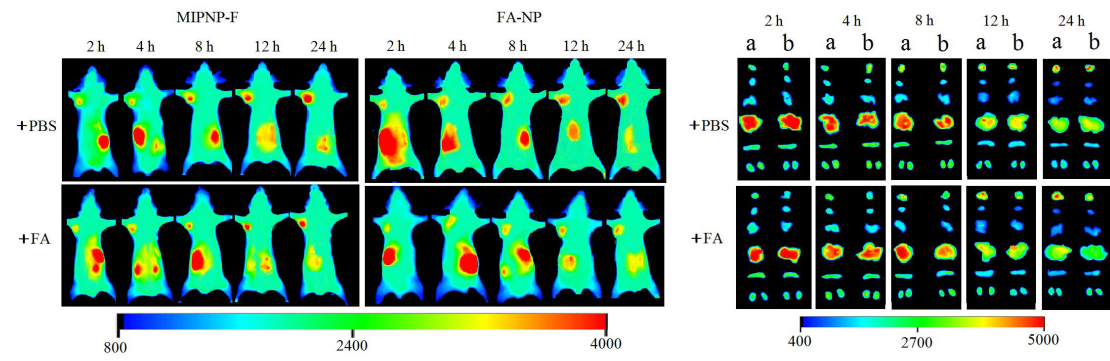


Figure S16. The potential influence of free FA on the targeting ability of MIPNP-F or FA-NP in HeLa- tumor-bearing nude mice.

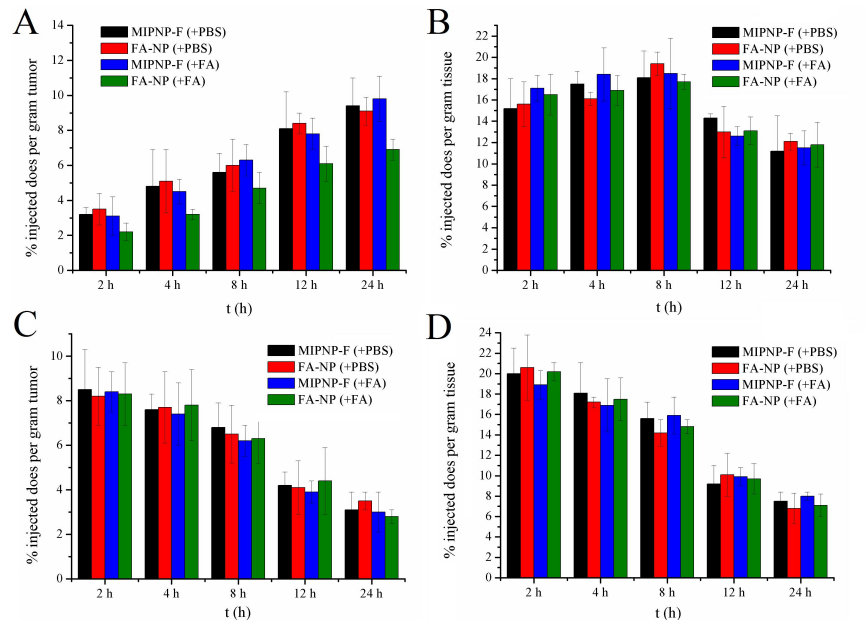


Figure S17. In vivo (HeLa-tumor-bearing nude mice) quantitative results of the tissue distribution of C6-loaded MIPNP-F or FA-NP in the case of pre-injection of free FA near the tumor. Fluorescence distribution in the tumor(A) , kidneys (B), liver (C), and spleen (D) at different time points. (n=6)

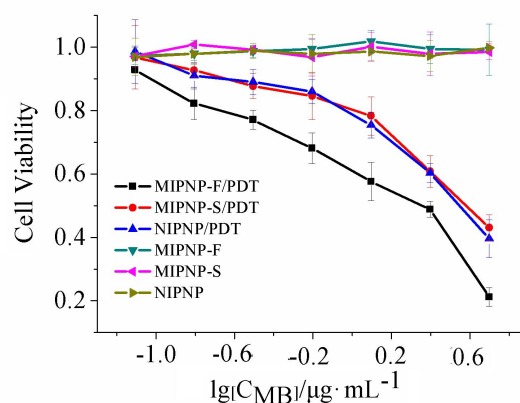


Figure S18. Cytotoxic effect of MB-loaded NPs (MIPNP-F, MIPNP-S, NIPNP) on HeLa cells, studied using PDT. Cells were incubated with indicated concentrations of MB-loaded NPs for 2 h, following which the medium was refreshed and the cells were treated with a 650-nm laser at a total fluence of $36 \text{ J}\cdot\text{cm}^{-2}$. Cell viability was measured by the MTT assay. The IC_{50} of MB was $2.12 \mu\text{g}\cdot\text{mL}^{-1}$ in the MIPNP-F-treatment group and was $3.96 \mu\text{g}\cdot\text{mL}^{-1}$ in the NIPNP-treatment group.

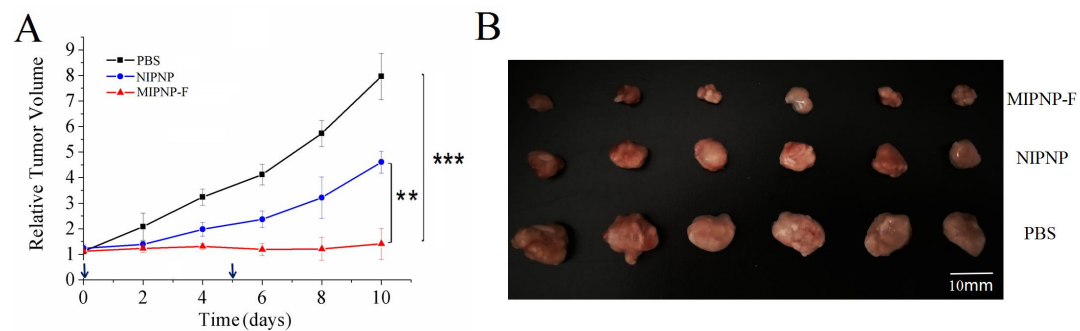


Figure S19. In vivo antitumor study conducted using PDT. (A) Relative tumor volumes were obtained for HeLa-tumor-bearing nude mice treated with MB-loaded NPs (MIPNP-F, MIPNP-S, NIPNP); **p < 0.01 and ***p < 0.005. (B) Photographs showing the morphology of the tumor xenografts in different groups.

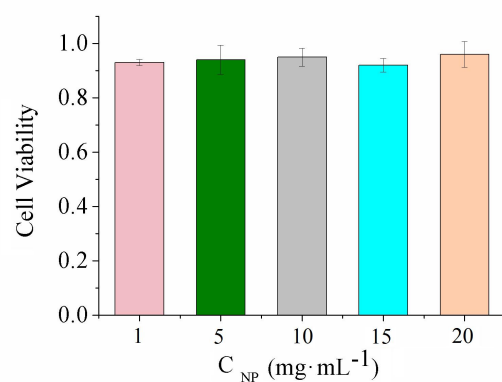


Figure S20. In vitro cytotoxicity of MIPNP-F in HeLa cells. MIPNP-F at indicated concentrations was added to cells and incubated for 72 h at 37 °C, and then cell viability was measured by the MTT assay.

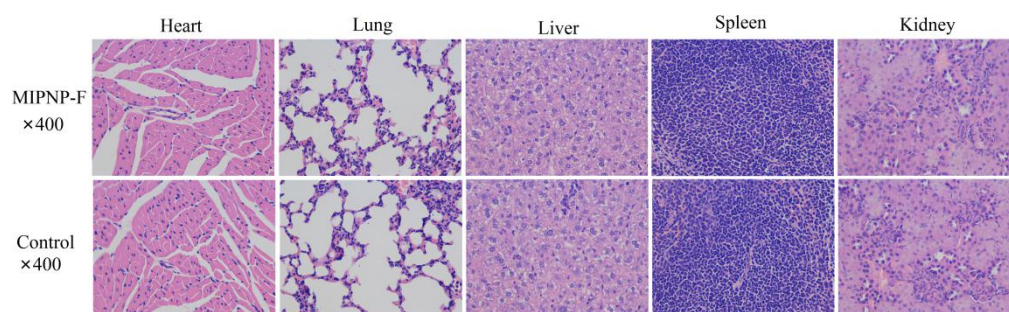


Figure S21. Tissue sections examined for in vivo toxicity of MIPNP-F. Hearts, livers, spleens, lungs, and kidneys were obtained at 10 days after intravenous injection of MIPNP-F or physiological saline. Organ sections were stained with H&E and examined at 400× magnification.

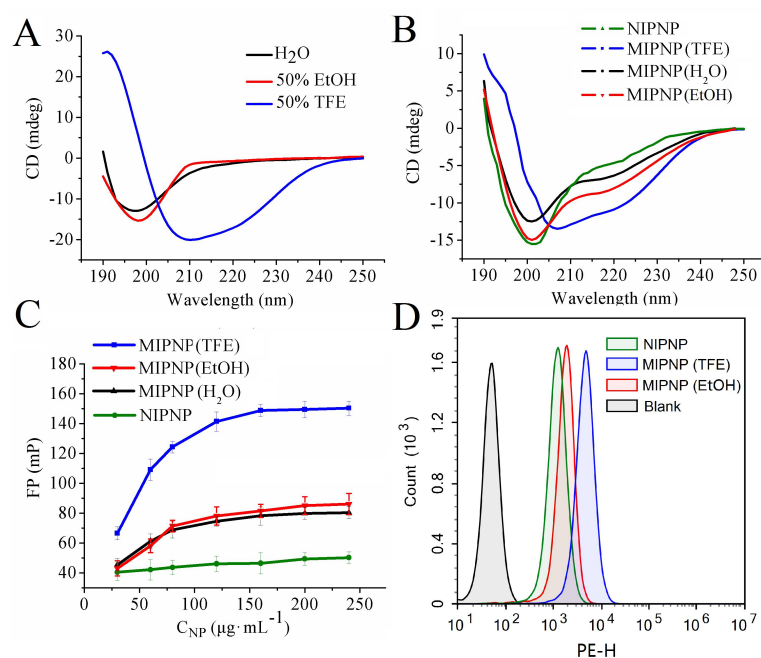


Figure S22. (A) CD spectrum of FN peptide in different solvents at 25°C. (B) Room-temperature CD spectra of FN peptide incubated with different NPs. (C) Direct binding between FN peptide and MIPNP (TFE), MIPNP (EtOH), MIPNP (H₂O) or NIPNP. (D) Flow cytometric measurement of the uptake of NIL-loaded NPs by Hela cells. Blank (black curves): the cells alone. MIPNP (TFE), MIPNP (EtOH), MIPNP (H₂O) refer to the nanoparticles prepared in 50% 2,2,2-trifluoroethanol, 50% ethyl alcohol, and pure water, respectively.